




A Plant Bacterial Pathogen Manipulates Its Insect Vector's Energy Metabolism

 Nabil Killiny,^a Faraj Hijaz,^a Timothy A. Ebert,^b Michael E. Rogers^b

Plant Pathology Department, Citrus Research and Education Center, University of Florida, Lake Alfred, Florida, USA^a; Entomology and Nematology Department, Citrus Research and Education Center, University of Florida, Lake Alfred, Florida, USA^b

ABSTRACT Insect-transmitted plant-pathogenic bacteria may alter their vectors' fitness, survival, behavior, and metabolism. Because these pathogens interact with their vectors on the cellular and organismal levels, potential changes at the biochemical level might occur. "*Candidatus Liberibacter asiaticus*" (CLas) is transmitted in a persistent, circulative, and propagative manner. The genome of CLas revealed the presence of an ATP translocase that mediates the uptake of ATP and other nucleotides from medium to achieve its biological processes, such as growth and multiplication. Here, we showed that the levels of ATP and many other nucleotides were significantly higher in CLas-infected than healthy psyllids. Gene expression analysis showed upregulation for ATP synthase subunits, while ATPase enzyme activity showed a decrease in ATPase activity. These results indicated that CLas stimulated *Diaphorina citri* to produce more ATP and many other energetic nucleotides, while it may inhibit their consumption by the insect. As a result of ATP accumulation, the adenylated energy charge (AEC) increased and the AMP/ATP and ADP/ATP ratios decreased in CLas-infected *D. citri* psyllids. Survival analysis confirmed a shorter life span for CLas-infected *D. citri* psyllids. In addition, electropenetrography showed a significant reduction in total nonprobing time, salivation time, and time from the last E2 (phloem ingestion) to the end of recording, indicating that CLas-infected psyllids were at a higher hunger level and they tended to forage more often. This increased feeding activity reflects the CLas-induced energetic stress. In conclusion, CLas alters the energy metabolism of its psyllid vector, *D. citri*, in order to secure its need for energetic nucleotides.

IMPORTANCE Insect transmission of plant-pathogenic bacteria involves propagation and circulation of the bacteria within their vectors. The transmission process is complex and requires specific interactions at the molecular and biochemical levels. The growth of the plant-pathogenic bacteria in the hemolymph of their vectors indicated that the hemolymph contains all the necessary nutrients for their growth. In addition to nutrients, "*Candidatus Liberibacter asiaticus*" (CLas) can take up energetic nucleotides, such as ATP, from its vector, *Diaphorina citri*, using ATP translocase. In this study, we found that the CLas pathogen manipulates the energy metabolism of its insect vector. The accumulation of ATP in CLas-infected *D. citri* psyllids indicated that CLas induces ATP production to fulfill its need for this energetic compound. As a result of ATP accumulation, a shorter life span and altered feeding behavior were observed. These findings increase our knowledge of insect transmission of the persistent-circulative-propagative type of plant pathogens vectored by insects.

KEYWORDS huanglongbing, *Diaphorina citri*, "*Candidatus Liberibacter asiaticus*," energy metabolism, ATP, adenylated energy charge, HPLC, electric penetration graph, electropenetrography

Received 30 October 2016 Accepted 19 December 2016

Accepted manuscript posted online 30 December 2016

Citation Killiny N, Hijaz F, Ebert TA, Rogers ME. 2017. A plant bacterial pathogen manipulates its insect vector's energy metabolism. *Appl Environ Microbiol* 83:e03005-16. <https://doi.org/10.1128/AEM.03005-16>.

Editor Harold L. Drake, University of Bayreuth

Copyright © 2017 American Society for Microbiology. All Rights Reserved.

Address correspondence to Nabil Killiny, nabilkilliny@ufl.edu.

Insect vectors transmit a variety of pathogens to a wide range of animal and plant hosts (1). Human vector-borne diseases account for more than 17% of the total infectious diseases every year (2). Malaria, the most important vector-borne disease, causes 1 to 3 million deaths per year (2). In addition, vector-borne diseases can cause huge economic losses when they attack livestock and crops (2). Huanglongbing, citrus tristeza, and citrus stubborn disease are examples of economically important plant vector-borne diseases in the citrus agroecosystem (3). Studying vector-pathogen-host relationships is essential to understanding the epidemiology of many important plant diseases (2).

The interaction between bacteria and their insect vectors can be mutualistic, parasitic, or commensal, depending on the relative effects of the bacteria on the fitness of the insect (4). Most of the previous studies about the interactions between the bacteria and their insect vectors showed that animal pathogens were virulent to their vectors whereas plant pathogens were beneficial to their vectors (4). Because most of the studies that demonstrated positive effects did not focus on the direct consequences of the plant pathogens to vector fitness, the results obtained from these studies could be biased (4). On the other hand, a number of studies demonstrated that some plant pathogens were virulent to their vector (5, 6). Nachappa et al. (4) showed that there was a negative relationship between "*Candidatus Liberibacter solanacearum*" level and the fecundity of its psyllid vector (*Bactericera cockerelli* [Šulc] [Hemiptera: Trioziidae]). Interestingly, "*Ca. Liberibacter solanacearum*" did not affect the mortality index of adult psyllids (6).

Studying the effect of plant pathogens on the fitness of their vector is difficult, because many of these pathogens cannot be cultured *in vitro* (5). The number of studies that focused on the effects of phytopathogens on the fitness of their insect vectors is limited, and only a few systems have been studied (5, 6). Furthermore, information about the effect of "*Candidatus Liberibacter asiaticus*" (CLAs), the causal agent of citrus greening, on its insect vector (*Diaphorina citri*) is limited.

Citrus greening, also known as huanglongbing (HLB), is currently threatening the citrus industry worldwide. HLB was first identified in China in the beginning of the 20th century and has been recently identified in Brazil and Florida (7). The CLAs bacterium, which is associated with HLB, is a phloem-restricted Gram-negative bacterium that has not yet been cultured (8). Three species of the causal agent have been associated with HLB: "*Candidatus Liberibacter asiaticus*" (Asia, North America, and Brazil), "*Candidatus Liberibacter africanus*" (Africa), and "*Candidatus Liberibacter americanus*" (Brazil) (9). CLAs and "*Candidatus Liberibacter americanus*" are transmitted by the Asian citrus psyllid, *Diaphorina citri* Kuwayama (Hemiptera: Liviidae), whereas "*Ca. Liberibacter africanus*" is transmitted by the African citrus psyllid, *Trioza erytreae* (Del Guercio) (Hemiptera: Trioziidae) (10). *D. citri* has received great attention in the past few years, and its transcriptomes (egg, nymph, and adult) were characterized (11).

CLAs has a relatively small genome (~1.2 Mbp), and it is an obligate intracellular pathogen (12). Genome sequencing of CLAs revealed that CLAs is not able to synthesize tryptophan, tyrosine, leucine, isoleucine, and valine from metabolic intermediates (13). Consequently, the CLAs bacterium counters these deficiencies by importing these amino acids from its host (14). The genome sequencing of CLAs also revealed that it cannot synthesize fumarate, malate, succinate, and aspartate because it lacks an isocitrate lyase and malate synthase (13). CLAs needs to acquire these intermediates from its host (14).

CLAs encodes >100 proteins, with 92 genes that are involved in active transport, and 40 of these genes are ATP binding cassette (ABC) transporter genes (14). Analysis of these ABC transporter-related proteins by Li et al. (15) showed that CLAs can use them to import metabolites and enzyme cofactors (14). It is also thought that the presence of this large number of transporter proteins might play an important role in providing CLAs with the nutrients necessary for growth and reproduction (14).

CLAs encodes ATP synthase, ATPase, and ATP/ADP translocase, which means that CLAs can synthesize its own ATP or utilize it directly from its host (13). To test this

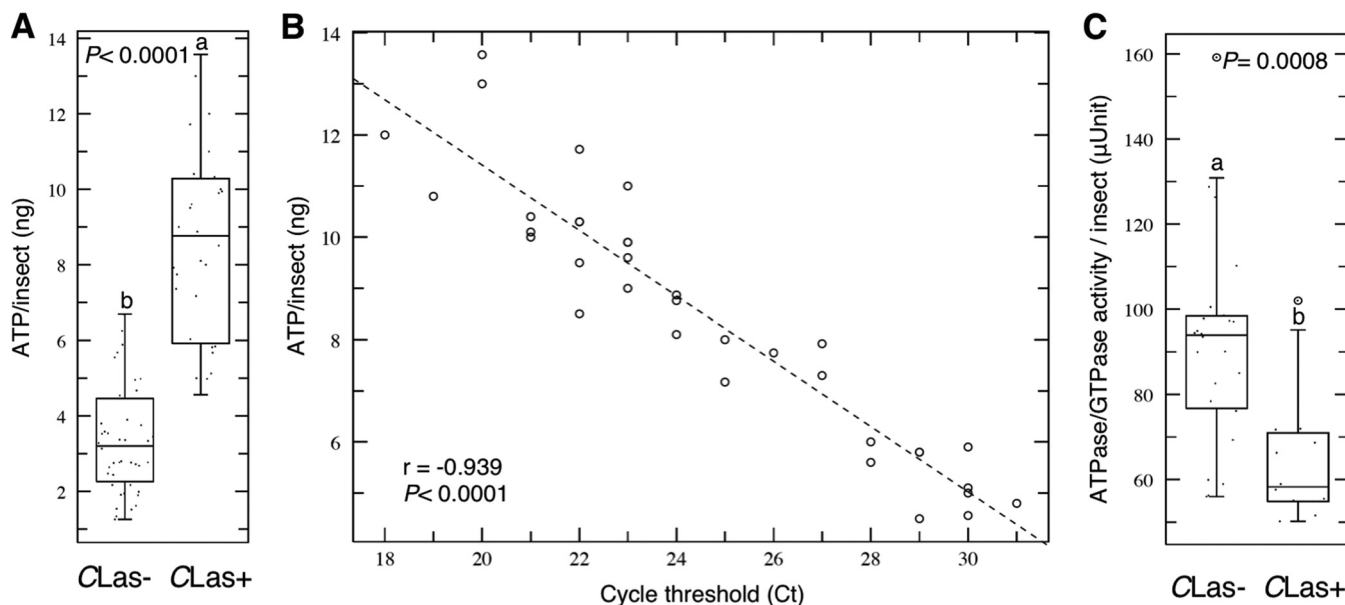


FIG 1 (A) Enzymatic quantification of ATP. (B) Simple linear regression plot of the ATP level versus the cycle threshold (C_T) of real-time PCR for the detection of CLas. (C) Total ATPase/GTPase activity in CLas-infected (CLas+) and healthy (CLas-) *Diaphorina citri* psyllids. For panels A and C, horizontal thick lines indicate the medians, boxes show the interquartile ranges including 25 to 75% of the values, and whiskers show the highest and the lowest values in each set. The circles represent outliers. Letters on the bars indicate significant differences ($P \leq 0.05$).

hypothesis, Vahling et al. (16) expressed the ATP translocase nucleotide transport protein (NttA) gene contained in CLas in *Escherichia coli*. *E. coli* harboring the NttA gene was able to import exogenous ATP directly into the cell. Vahling et al. (16) concluded that some intracellular bacteria of plants have the potential to import ATP from their environment.

Interestingly, it has been shown that the antigenic membrane protein of "*Candidatus* Phytoplasma asteris" interacts with the ATP synthase of its leafhopper vectors (17). Because the phytoplasmas lack the ATP synthetic pathway and depend partly on their host for energy, it has been suggested that host extracellular ATP in the gut lumen and hemocoel may be required for the survival of phytoplasmas (17). Vahling et al. (16) also suggested that the addition of external ATP to the culture medium might facilitate the growth of the CLas bacterium *in vitro*.

In the current study, we hypothesize that the bacterial pathogen CLas alters the energy metabolism of its insect vector, the Asian citrus psyllid, in order to meet its needs for energetic nucleotides, mainly ATP. We also hypothesize that the bacterium may stimulate the insect to overproduce and/or inhibit its utilization of the energetic nucleotides. The accumulated ATP in the insect would be translocated to the bacterial cell by ATP/ADP translocase.

RESULTS

Infection with CLas increased the ATP level in *D. citri*. Enzymatic quantification showed that the level of ATP in CLas-infected *D. citri* psyllids was significantly higher than that in the controls (Fig. 1A). The quantity of ATP in control psyllids was between 2 to 5 ng/insect, whereas it ranged from 4 to 14 ng/insect in CLas-infected psyllids. This result indicates that the amount of ATP was affected by the presence of the CLas bacterium.

Level of ATP was dependent on the CLas population. The linear regression of the levels of ATP versus the cycle threshold (C_T) value for healthy psyllids did not show any correlation between ATP level and C_T value (data not shown). On the other hand, the linear regression of the levels of ATP versus the C_T value showed a significant negative relationship between ATP level and C_T value (Fig. 1B). In other words; there was a significant positive density-dependent relationship between CLas cells and ATP content

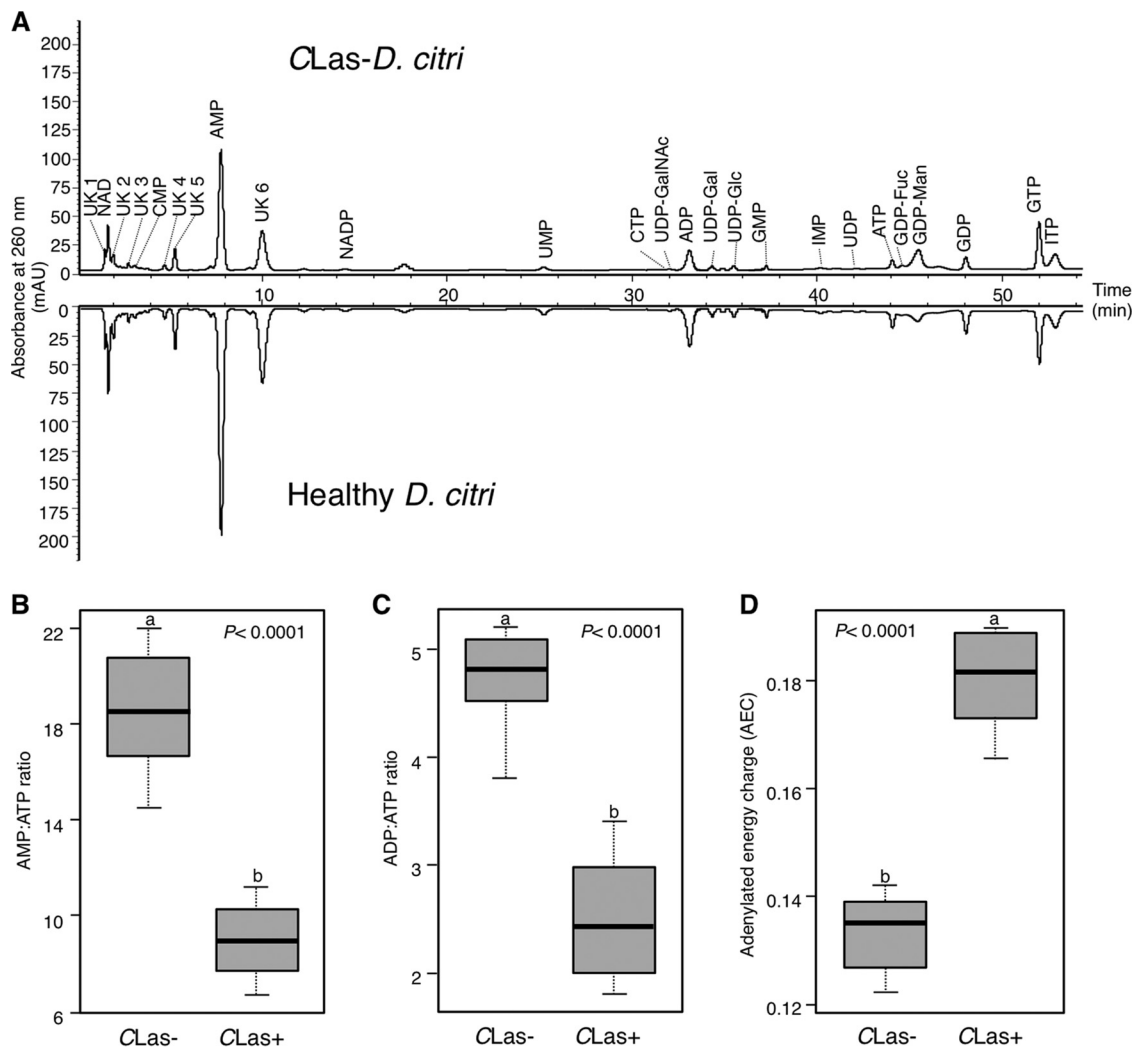


FIG 2 Mirror high-performance anion-exchange chromatograms of nucleotides and sugar nucleotides detected in healthy (CLas⁻) and CLas-infected (CLas⁺) *Diaphorina citri* adults. (B to D) AMP/ATP ratios (B), ADP/ATP ratios (C), and adenylylated energy charge (AEC) values (D) in healthy and CLas-infected *Diaphorina citri* adults. For panels B to D, horizontal thick lines indicate the medians, boxes show the interquartile ranges including 25 to 75% of the values, and whiskers show the highest and the lowest values in each set. Letters on the bars indicate significant differences ($P \leq 0.05$).

in CLas-infected *D. citri* psyllids. This correlation confirmed that the increase in ATP level was due to the presence of CLas.

Infection with CLas decreased ATPase/GTPase activity in *D. citri*. ATPase/GTPase activity was significantly reduced (P value = 0.0008) in CLas-infected psyllids compared to that in the control (Fig. 1C). The ATPase/GTPase level (mean \pm SD) in control psyllids was 93 ± 32 μ U/insect, whereas it was 67 ± 23 μ U/insect in CLas-infected psyllids.

Infection by CLas altered the nucleotide profile of its vector. Eighteen nucleotides, four sugar nucleotides, and five unknowns were detected in the perchloric acid extracts of *D. citri* (Fig. 2A). In agreement with the Enliten ATP kit's result, the high-performance liquid chromatography (HPLC) results (Table 1) showed that the ATP level in CLas-infected psyllids was significantly higher than in the controls. In addition to ATP, the levels of AMP, UMP, ADP, UDP-Glc, GMP, UDP, ATP, GDP, unknown 2 (UK2), UK3, and UK4 in CLas-infected psyllids were significantly higher than those in the controls. The levels of CMP, UDP-GalNAc, UDP-Gal, GDP-F, and UK1 were also higher, but not significantly so. On the other hand, the level of GDP-Man in CLas-infected psyllids was significantly lower than in the controls. The reduction in GDP-Man in CLas-infected psyllids indicated that GDP-Man could be essential for the survival of the CLas bacterium. Slight reductions in NADP and IMP levels were also observed.

TABLE 1 Nucleotide and sugar nucleotide concentrations in healthy and CLas-infected Asian citrus psyllids

Nucleotide or sugar nucleotide	Abbreviation	Concn (mean \pm SD) (μ g/insect) ^a	
		Healthy ACP	CLas-infected ACP
Unknown 1	UK1	0.055 \pm 0.032 A	0.113 \pm 0.049 A
Beta-NAD hydrate	NAD	0.095 \pm 0.046 A	0.155 \pm 0.067 A
Unknown 2	UK2	0.020 \pm 0.012 B	0.074 \pm 0.013 A
Unknown 3	UK3	0.008 \pm 0.002 B	0.025 \pm 0.008 A
Cytidine 5'-monophosphate	CMP	0.009 \pm 0.003 A	0.048 \pm 0.036 A
Unknown 4	UK4	0.012 \pm 0.001 B	0.032 \pm 0.013 A
Unknown 5	UK5	0.069 \pm 0.020 A	0.084 \pm 0.004 A
Adenosine 5'-monophosphate	AMP	0.549 \pm 0.116 B	0.970 \pm 0.082 A
Unknown 6	UK6	0.268 \pm 0.049 A	0.389 \pm 0.059 A
B-NADP, oxidized form	NADP	0.068 \pm 0.025 A	0.065 \pm 0.004 A
Cytidine 5'-diphosphate	CDP	ND	ND
Uridine 5'-monophosphate	UMP	0.036 \pm 0.010 B	0.079 \pm 0.017 A
Cytidine 5'-triphosphate	CTP	0.019 \pm 0.006 B	0.024 \pm 0.003 A
Uridine 5'-diphospho-N-acetyl-D-galactosamine	UDP-GalNAc	0.029 \pm 0.016 A	0.077 \pm 0.032 A
Adenosine 5'-diphosphate	ADP	0.141 \pm 0.038 B	0.252 \pm 0.028 A
Uridine 5'-diphospho-N-acetyl-D-glucosamine	UDP-GlcNAc	ND	ND
Uridine 5'-diphospho-D-galactose	UDP-Gal	0.002 \pm 0.001 A	0.009 \pm 0.007 A
Uridine 5'-diphospho-D-glucose	UDP-Glc	0.018 \pm 0.012 B	0.057 \pm 0.009 A
Guanosine 5'-monophosphate	GMP	0.033 \pm 0.017 B	0.090 \pm 0.025 A
Inosine 5'-monophosphate	IMP	0.009 \pm 0.003 A	0.008 \pm 0.004 A
Uridine 5'-diphosphate	UDP	0.005 \pm 0.001 B	0.019 \pm 0.004 A
Adenosine 5'-triphosphate	ATP	0.029 \pm 0.008 B	0.108 \pm 0.017 A
Guanosine 5'-diphosphate-beta-L-fucose	GDP-Fuc	0.014 \pm 0.002 A	0.085 \pm 0.045 A
Guanosine 5'-diphosphate-D-mannose	GDP-Man	0.332 \pm 0.083 A	0.063 \pm 0.011 B
Uridine 5'-triphosphate	UTP	ND	ND
Guanosine 5'-diphosphate	GDP	0.051 \pm 0.011 B	0.079 \pm 0.021 A
Inosine 5'-diphosphate	IDP	ND	ND
Flavin adenine dinucleotide	FAD	ND	ND
Guanosine 5'-triphosphate	GTP	0.278 \pm 0.04 A	0.304 \pm 0.06 A
Inosine 5'-triphosphate	ITP	0.181 \pm 0.04 A	0.184 \pm 0.01 A

^aACP, Asian citrus psyllids; ND, nondetected compound. Numbers that are followed by the same letters do not show significant differences ($P < 0.05$).

CLas altered the energy homeostasis of its insect vector. CLas infection changed the level of many nucleotides in *D. citri*, thereby altering the nucleotide ratios used to measure cellular energy balance. CLas infection significantly decreased the ratios of AMP/ATP (Fig. 2B) and ADP/AMP (Fig. 2C). The ratios of AMP/ATP and ADP/ATP in CLas-infected psyllids were about half of those of the controls. On the other hand, the adenylated energy charge (AEC) of CLas-infected psyllids was significantly higher than that of the control (Fig. 2D). These results showed that CLas significantly alters the energy homeostasis of its vector.

CLas increased ATP synthesis and decreased its breakdown in its insect vector.

The gene expression analysis showed that the levels of expression of ATP synthase mitochondrion-like alpha/beta subunits (ATP synthase α/β -subunits) were upregulated in CLas-infected psyllids (Fig. 3). On the other hand, the levels of expression of the V-type proton ATPase catalytic subunit A (V-ATPase-V1a) and transitional endoplasmic reticulum ATPase (TER94) genes in CLas-infected psyllids were reduced compared to those in the controls (Fig. 3). In addition, the level of expression of the nucleotide diphosphate kinase (NDPK) gene in CLas-infected *D. citri* psyllids was increased, whereas expression of the AMP-activated protein kinase α subunit (AMPK-A) gene was significantly reduced in CLas-infected psyllids (Fig. 3).

CLas shortened the life span of its vector. Survival analysis using the Kaplan-Meier method showed that CLas decreased the survival probability (Fig. 4A) and the life span (Fig. 4B) of its vector, *D. citri*. Since the survival assay was carried out using an artificial diet system, this result suggested that CLas was directly responsible for the reduced life span.

CLas-infected psyllids were more susceptible to hunger than healthy psyllids.

Characteristic electrical penetration graph (EPG) waveforms produced by *D. citri* on

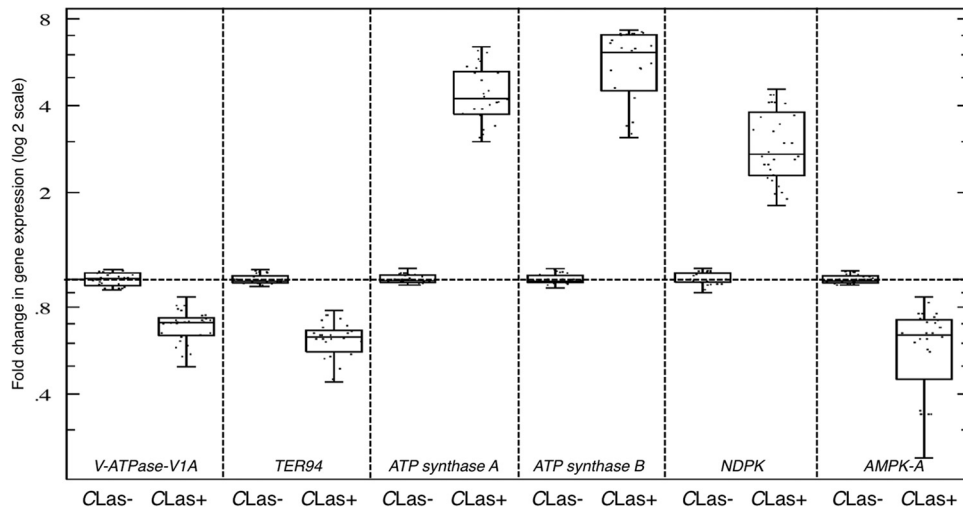


FIG 3 Expression of genes encoding ATP synthase mitochondrion-like alpha/beta subunits (ATP synthase α/β -subunits), V-type proton ATPase catalytic subunit A (V-ATPase-V1a), transitional endoplasmic reticulum ATPase (TER94), nucleotide diphosphate kinase (NDPK), AMP-activated protein kinase α -subunit (AMPK-A) in CLas-infected (CLas+) and healthy (CLas-) *Diaphorina citri* psyllids. Horizontal thick lines indicate the medians, boxes show the interquartile ranges including 25 to 75% of the values, and whiskers show the highest and the lowest values in each set.

leaves of Midsweet orange with enlargements and a detailed view of each waveform are shown in Fig. 5A and B. The EPG data showed that there was no significant difference in the phloem phase (E2) or xylem phase (G) between CLas-infected and healthy psyllids (Table 2). The numbers of phloem probing phases and xylem probing phases and the proportions of time spent on each phase were also similar (Table 2). On the other hand, the durations of the total nonprobing period and the time from the last E2 to the end of recording (TmLstE2EndRcrd) in CLas-infected psyllids were significantly shorter than those of the controls ($27,606 \pm 2,675$ and $12,416 \pm 1,158$ [CLas-infected psyllids], respectively, and $32,696 \pm 1,985$ and $39,170 \pm 1,637$ [healthy psyllids] respectively). In addition, the salivation time in CLas-infected psyllids was significantly lower than that of the controls (Table 2). These observations together suggested that CLas-infected psyllids were at a higher hunger level, and they tended to look for more food.

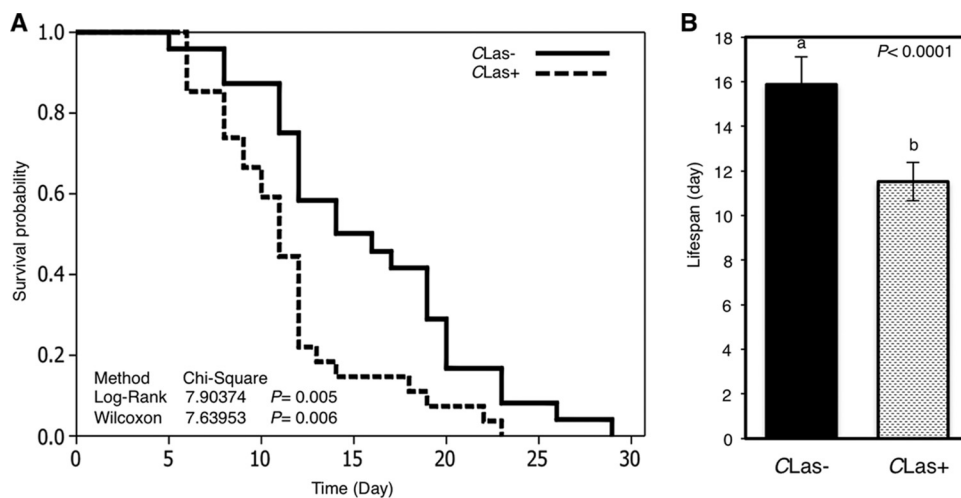


FIG 4 (A) Kaplan-Meier analysis of survival of healthy (CLas-) and CLas-infected (CLas+) *Diaphorina citri* adults carried out with a 20% sucrose solution. The log-rank and Wilcoxon values were used to compare survival curves. (B) The average life spans for CLas-infected and healthy *Diaphorina citri* psyllids. Bars represent standard errors. Letters on the bars indicate significant differences ($P \leq 0.05$).

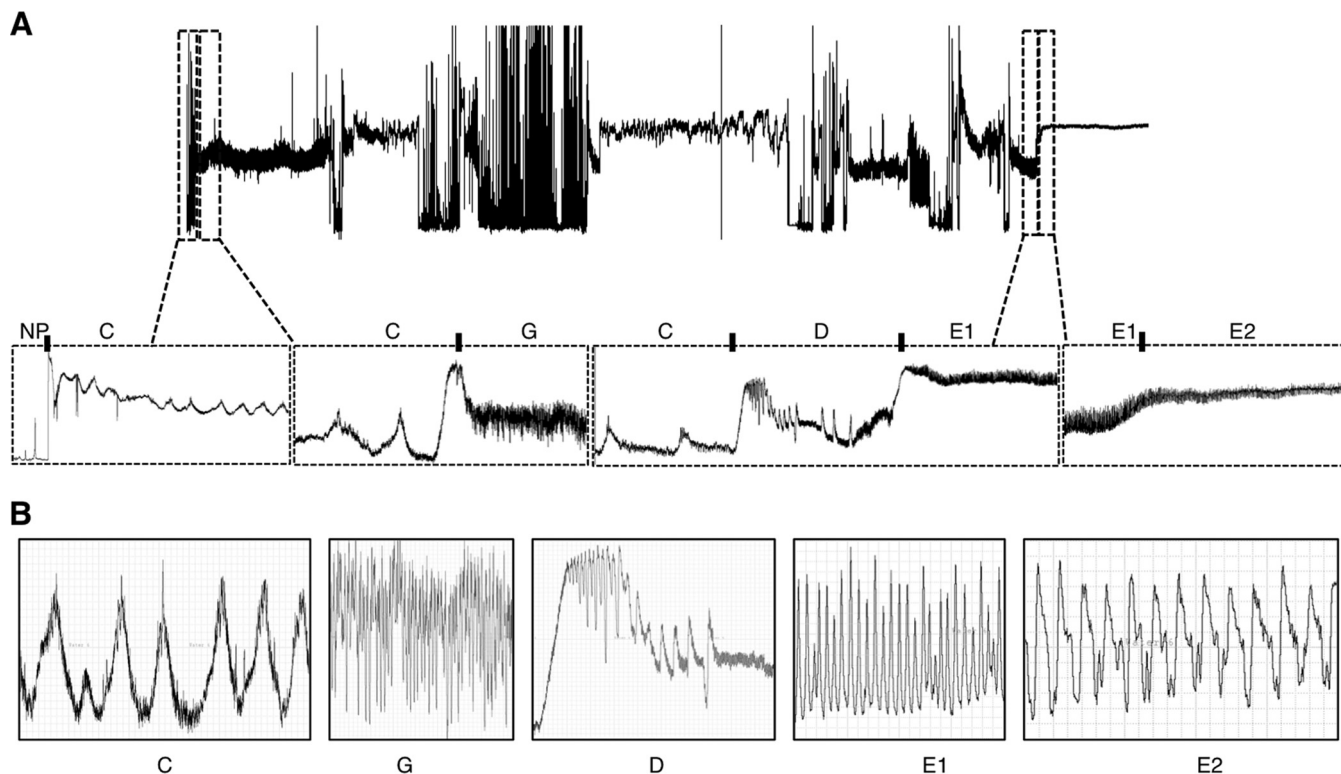


FIG 5 (A) General (24-h) scheme of characteristic electrical penetration graph (EPG) waveforms produced by *Diaphorina citri* on leaves of Midsweet orange, *Citrus sinensis*, with enlargements of specific waveforms showing nonprobing (NP) pathway (C), xylem ingestion (G), contact with phloem (D), salivation into the phloem (E1), and phloem ingestion (E2). (B) Detailed view of each waveform showing characteristic patterns of each waveform.

DISCUSSION

Our results showed that CLas infection shortened the life span of Asian citrus psyllids, and this was accompanied by a decrease in AMP/ATP and ADP/ATP ratios. In agreement with the current results, we have recently found that adult *D. citri* survival under different temperatures was positively correlated with AMP/ATP and ADP/ATP

TABLE 2 Selected EPG variables associated with ingesting xylem or phloem along with three variables that showed a difference in behavior between healthy and CLas-infected psyllids on plants^a

Variable name	CLas-infected psyllids			Healthy psyllids			F	Pr > F
	n	Mean	SD	n	Mean	SD		
NumG	25	5.52	4.86	27	6.19	4.04	0.29	0.5926
MeanG	25	1,757.7	1,681.0	27	1,383.5	675.5	1.14	0.2907
PrcntPrbG	25	18.53	20.01	27	16.58	10.10	0.01	0.9232
NumE2	25	2.08	3.00	27	1.59	1.91	0.1	0.7581
NumLngE2	25	1.68	2.30	27	1.41	1.67	0.03	0.8596
MnDurE2	14	5,463.2	2,242.7	16	9,402.7	9,888.7	1.77	0.1944
MaxE2	14	8,912.4	3,702.3	16	10,976.2	9,155.3	0.43	0.5157
PrcntPrbE2	25	15.72	17.88	27	20.89	22.08	0.37	0.5435
DurNnprbBfrFrstD	15	9,659.6	6,619.3	18	19,327.4	10,892.2	9.69	0.004
DurE1FlwdFrstSusE2	14	22.07	21.85	16	72.92	76.53	6.3	0.0181
DurE1FlldFrstE2	14	25.65	22.69	16	72.47	76.88	4.55	0.0418

^aNumG, number of xylem ingestion events; MeanG, mean duration of xylem ingestion; PrcntPrbG, percentage of probing duration spent in xylem ingestion; NumE2, number of phloem ingestion events; NumLngE2, number of phloem ingestion events longer than 600 s; MnDurE2, mean duration of E2; MaxE2, longest recorded E2 for each insect; PrcntPrbE2, percentage of probing duration spent ingesting phloem; DurNnprbBfrFrstD, duration of nonprobing period before first phloem contact; DurE1FlwdFrstSusE2, duration of the phloem salivation event before first sustained (600+ s) phloem ingestion event; DurE1FlldFrstE2, duration of the phloem salivation event immediately before the first phloem ingestion event. All variables were calculated by insect, and the mean values are reported. Pr > F, the probability of a greater F statistic value under the null hypothesis.

ratios (18). Colinet (19) also found that the higher level of ATP was observed in lesser mealworm beetles (*Alphitobius diaperinus*) during chronic cold stress. Stenesen et al. (20) showed that heterozygous mutations of AMP biosynthetic enzymes extend *Drosophila* life span by increasing AMP/ATP and ADP/ATP ratios and the activity of AMPK. Apfeld et al. (21) and Curtis et al. (22) showed that increased AMPK activity due to increased AMP/ATP ratio also elongated the life span of the nematode *Caenorhabditis elegans*.

The increase in the adenylated energy charge (AEC) in CLas-infected psyllids was also correlated with a reduction in the life span and survival of *D. citri*. Interestingly, our recent study also showed that the AEC of *D. citri* was negatively correlated with adult psyllid survival (23). In agreement with our results, AEC was also negatively correlated with the survival of other species. Marazza et al. (24) showed that the AEC of shrimp (*Palaemonetes varians*) was increased upon exposure to lethal levels (3 mg/liter) of ammonia. An increase in AEC was also observed in other inhabitants of polluted seawater (25, 26).

Adenine nucleotides play important roles in metabolic regulation, and the mechanism of life span extension involves an increase in AMP/ATP and ADP/ATP ratios (20). Hydrolysis of ATP in tissues produce ADP, while AMP is produced by the reaction catalyzed by adenylate kinase ($2 \text{ ADP} \leftrightarrow \text{ATP} + \text{AMP}$) (27). The activity of many metabolic enzymes, including glycogen phosphorylase and 6-phosphofructo-1-kinase in muscle, responds to the AMP/ATP ratio (27). An increase in AMP/ATP ratios activates both glycogen phosphorylase and 6-phosphofructo-1-kinase and consequently switches on glycogenolysis and glycolysis (3). High AMP/ATP ratios inhibit fructose-1,6-bisphosphatase activity in the liver and switch off the anabolic pathway, gluconeogenesis (27). In addition, the increase in ADP/ATP and AMP/ATP ratios activates the AMPK energy sensor, which regulates all aspects of cell function, including energy homeostasis (27).

CLas increased ATP levels in *D. citri*, and this increase was accompanied by an increase in the gene expression of NDPK and a decrease in AMPK. Onyenwoke et al. (28) demonstrated that AMPK and NDPK genetically antagonize each other (Fig. 6). Under nutrient-rich conditions (high ATP level), AMPK is inactive, while NDPK is active and consumes ATP to produce other nucleotides in order to maintain cellular homeostasis (Fig. 6) (28). On the other hand, during starvation (low ATP level), AMPK is active and inhibits NDPK activity (Fig. 6) (28). The increase in NDPK expression in CLas-infected *D. citri* psyllids could be an attempt to maintain cellular homeostasis (Fig. 6). Failure to maintain cellular homeostasis and the decrease in AMPK activity disrupts many aspects of cellular function and results in cell death (28). In addition, overexpression of NDPK in *Drosophila* spp. led to a decrease in their survival under starvation conditions (29). The increase in NDPK activity and the decrease in AMPK may explain the shorter life span observed in CLas-infected psyllids.

Taken together, the current results suggested that CLas manipulates the energy metabolism of its insect vector to fulfill its need for energetic nucleotides. In other words, CLas increases the levels of ATP in its host insect in order to increase its availability and utilize it. The presence of ATP/ADP translocase in CLas (13) and the ability of *E. coli*, which encodes the CLas ATP translocase, to import exogenous ATP (16) support this hypothesis. CLas encodes both ATP synthase and ATP/ADP translocase, which means that CLas can synthesize its own ATP or utilize it directly from its host (13). However, it is still not clear which of them (ATP synthase or ATP/ADP translocase) contributes more to CLas energy. CLas could be like phytoplasmas, as it depends partly on its host for energy (17). Consequently, extracellular ATP in the gut lumen and hemocoel may also be required for CLas survival (17).

Parasites usually acquire nutrients from their host, and this results in energetic stresses in their host. Immunological responses of the host to the infectious agent are also energetically expensive, further increasing energetic stress (30). Mayack and Naug (31) showed that *Nosema ceranae* decreases the survival of its honeybee host (*Apis mellifera*) by inducing energetic stress. Feeding and extension experiments showed that

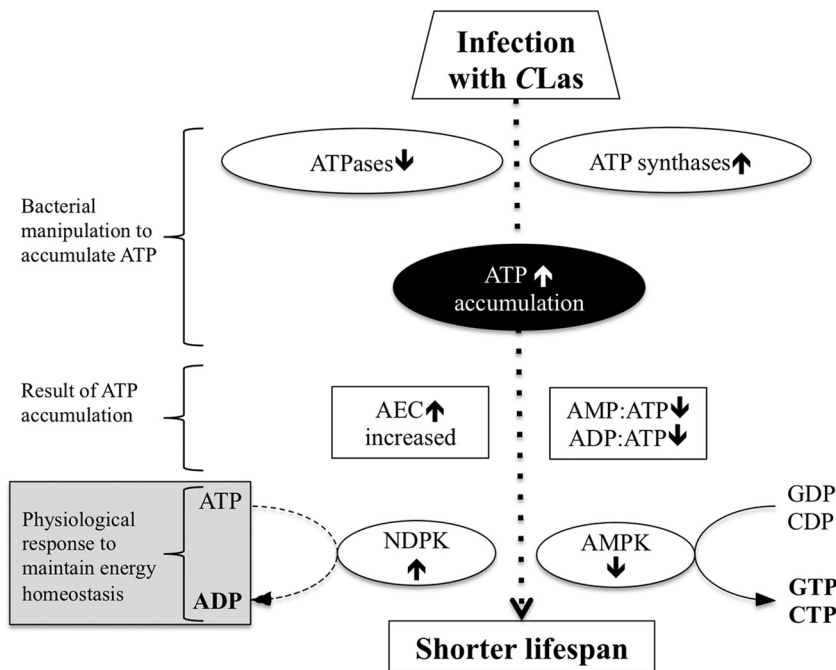


FIG 6 A hypothetical model for the decrease in life span in CLas-infected psyllids as a result of accumulation of ATP. Infection with CLAs enhances ATP accumulation and consequently increases adenylated energy charge (AEC) and decreases AMP/ATP and ADP/ATP ratios. As a result of the increase in AEC and the decrease in AMP/ATP and ADP/ATP ratios, the activity of AMPK will decrease and the activity of NDPK will increase in order to maintain energy homeostasis. Failure to maintain cellular homeostasis and the decrease in AMPK activity will disrupt many aspects of cellular functions and result in cell death and shorter life span in *D. citri*.

hunger levels of infected honeybees were higher than in uninfected honeybees (31). The metabolic profile of *N. ceranae*-infected honeybees showed a decline in most of the carbohydrates and amino acids (32). Because mitochondria are absent in *Nosema* species, Martín-Hernández et al. (33) suggested that they either consume ATP from their host or synthesize it by metabolizing carbohydrates present in their host. The accumulation of ATP in CLas-infected psyllids and the decrease in its life span indicated that CLas induces energetic stress in its vector. Since the CLas does not produce any known toxin and does not have any specialized secretion system or extracellular degrading enzymes, the pathogenicity of CLas could be due to metabolic imbalances caused by nutrient depletion and energy parasitism (13, 14, 16).

Recently, Martini et al. (34) found that CLas infection affected the behavior of *D. citri* by increasing dispersal and flight initiation; however, it did not affect duration and speed of flight. However, the reason behind the increase in dispersal and flight initiation in CLas-infected psyllids was not investigated in that study. We believe that the energetic stress and increased hunger level in CLas-infected psyllids could explain the observed increase in their dispersal and flight initiation. Energetic stress and hunger in *N. ceranae*-infected honeybees increased their foraging rates and consequently resulted in the disappearance of honeybee colonies (31). Our EPG data (the significant reduction in total nonprobing time, salivation time, and time from the last E2 to the end of recording) indicated that CLas-infected psyllids were at a higher hunger level.

Enhancement of ATP and glutamate synthesis was also observed in *Chlamydia psittaci*-infected HeLa cells (35). The increase in the expression of the glucose transporter (GLUT-1) on HeLa cells indicated that the stimulation of ATP was attributed to enhancement of glucose consumption by infected cells (35). Enhanced synthesis of ATP in infected cells could benefit both *Chlamydia* spp. and its host (35). In fact, *C. psittaci* can also take up external ATP via ADP/ATP translocase, and it was concluded that *C. psittaci* compensates for the energy load it imposes on infected cells by increasing the production of ATP and other high-energy metabolites (35).

The accumulation of ATP was accompanied by an increase in the gene expression of ATP synthase subunits and a decrease in ATPase/GTPase enzyme activity. Our comparative proteomic analyses of CLas-infected and healthy *D. citri* psyllids showed that the amounts of ATP synthase α/β -subunits were higher in CLas-infected psyllids (N. Killiny, unpublished data). On the other hand, our proteomic analyses showed that the level of V-ATPase-V1A was downregulated (unpublished data). In agreement with our results, proteins involved in metabolism and cellular energy storage and utilization were upregulated in CLas-infected *D. citri* psyllids (36). The acyl-coenzyme A (acyl-CoA) dehydrogenase and enoyl-CoA hydratase proteins, the enzymes catalyzing the first and the second steps in fatty acid β -oxidation and the production of acetyl-CoA, which feeds into the citric acid cycle, were highly upregulated (2-fold and 12-fold, respectively) in CLas-infected *D. citri* psyllids (36). A number of enzymes involved in the citric acid cycle were also upregulated in CLas-infected *D. citri* psyllids, including 2-oxoglutarate dehydrogenase, L-2-hydroxyglutarate dehydrogenase, phosphoglycerate mutase, succinate dehydrogenase, and succinate semialdehyde dehydrogenase (36). In addition, glycerol kinase, which is involved in triglyceride breakdown, and aldose-L-epimerase, which is involved in glycolysis, were upregulated in CLas-infected *D. citri* psyllids (36). In addition, the comparative transcriptomic analysis of CLas infection altered the expression of many genes involved in nutrient reservoir activity in *D. citri* (37). The gene expression results indicated that CLas alters its host environment to make the nutrients more available (37). Although our results showed that ATP synthesis was increased and its consumption was decreased in CLas-infected *D. citri* psyllids, the results indicated that the increased ATP synthesis may contribute more to the accumulation of ATP level than the decrease in consumption. Since CLas encodes ATP synthase, synthesis of ATP by CLas may also contribute to ATP accumulation in *D. citri*.

Our current study showed that CLas shortened the life span of its insect vector by exerting energy stress. By rearing CLas-infected psyllids on healthy plants, Pelz-Stelinski and Killiny (38) showed that the life span of CLas-infected *D. citri* psyllids was less than that of healthy psyllids. However, CLas infection also increased the fitness of adult psyllids, resulting in increased egg laying and faster development time (38). Pelz-Stelinski and Killiny (38) assumed that there was a physiological trade-off between reproduction and life span and concluded that CLas developed a relationship with *D. citri* before it moved to plants. In contrast to CLas, "*Ca. Liberibacter solanacearum*" reduces the fitness of its psyllid vector but does not affect its mortality index (6). Although the genomes of "*Ca. Liberibacter solanacearum*" and CLas are similar, these two pathogens are not identical at the molecular level (39). Recently, Gahnim et al. (39) showed observed apoptotic responses in the midgut of CLas-infected psyllids. Although the cause of this apoptosis response was not fully understood, it was hypothesized that it served to limit the acquisition and transmission efficiency of CLas (39). Better understanding of the interactions between CLas and its vector, *D. citri*, may help in creating new approaches for controlling HLB.

MATERIALS AND METHODS

Diaphorina citri colonies. Colonies of the Asian citrus psyllid *D. citri* were maintained on 'Valencia' sweet orange, *Citrus sinensis* L. Osbeck, inside 400-mesh rearing and observation cages (BioQuip, Rancho Dominguez, CA). Colonies were kept in temperature-controlled growth rooms set at $25 \pm 3^\circ\text{C}$, $60\% \pm 5\%$ relative humidity (RH), and with a 16:8 (light/dark) photoperiod. Originally, insects were collected in 2000 from citrus groves in Polk City, FL. For CLas-infected colonies, CLas-infected 'Valencia' sweet orange trees (symptomatic and PCR positive) were used to rear and maintain *D. citri* colonies. The infection rates were assessed using conventional PCR, as described below. When the infection rate reached 80 to 90%, insects were used for the survival analysis or collected and kept at -80°C for gene expression, enzymatic activity assays, and nucleotide analysis.

DNA extraction and conventional PCR for CLas. DNA from individual adult psyllids was extracted using potassium acetate buffer and a TissueLyser II (Qiagen, Valencia, CA). Briefly, an individual psyllid was placed in a 2-ml safe-lock microcentrifuge tube with a 5-mm-diameter stainless steel bead (Qiagen). The tubes were immersed in liquid nitrogen for up to 5 min and then were placed into the TissueLyser adaptor blocks (kept in the freezer) and fixed into the block clamps. Immediately, the samples were processed for 30 s at 30 Hz. The vibration was repeated three times with rotation of the adaptor blocks.

Eleven hundred microliters of extraction buffer (100 mM NaCl, 10 mM EDTA, 50 mM Tris [pH 9.0], 10 mM dithiothreitol [DTT]) was added to each tube, and brief centrifugation at 5,000 rpm for 1 min was performed to remove the debris. One milliliter of supernatant was recovered into a new 2-ml tube, and 20 μ l of 10% SDS was added. The mixture was incubated at 65°C in a water bath for 45 min; 500 μ l of 5 M potassium acetate was then added. After vortexing, the tubes were incubated in ice for 20 min and then were subjected to centrifugation at $16,595 \times g$ for 10 min at 4°C. One milliliter of supernatant was recovered and mixed with 1 ml of ice-cold isopropanol. The tubes were centrifuged again at high speed for 20 min at 4°C. After discarding the supernatant, 1 ml of ice-cold 70% ethanol was added to the pellet, and the tubes were well vortexed and centrifuged for 10 min at 4°C. Supernatant was pipetted carefully and discarded. DNA pellets were dried under a N₂ stream and were resuspended in 20 μ l of RNase-free water. The DNA concentration of each sample was measured using a NanoDrop ND1000 (Thermo Scientific). Extracted DNA was used for conventional PCR amplification using 16S rRNA gene primers O11 and I2C and Taq PCR master mix kit (Qiagen), as well as the protocol described by Jagoueix et al. (8).

ATP quantification by enzymatic assay. ATP was extracted using perchloric acid, as described by Tomiya et al. (40), with slight modification. In brief, one psyllid was placed in a 1-ml tube with 50 μ l of ice-cold 5% perchloric acid and crushed for 5 min in an ice bath using a Kontes mortar and pestle (Fisher Scientific, Pittsburgh, PA). The samples were centrifuged at $10,621 \times g$ for 10 min, and 4 μ l of the supernatant was diluted to 200 μ l using ATP-free water. The ATP assay was performed using the Enliten ATP kit (Promega, Madison, WI). Briefly, a 100- μ l aliquot of the diluted sample was mixed with 100 μ l of luciferase reagent, provided with the kit, in 12 by 75-mm polypropylene test tubes (Fisher Scientific), and the intensity of the emitted light was measured for 10 s using an Optocomp I luminometer (MGM Instruments). A set of ATP standards (1×10^{-8} to 1×10^{-12} M) were also prepared in 0.1% perchloric acid to correct for possible inhibition of light output and were used to construct the standard curve. A "blank" containing 100 μ l of luciferase reagent and 100 μ l of 0.1% perchloric acid was run in the assay to determine the amount of background relative luminescence units (RLU) to subtract from the sample RLU. Fifty healthy and 50 CLas-infected psyllids were analyzed, and each sample was measured in duplicate.

Bacterial cell quantification by real-time PCR for CLas. We carried out real-time quantitative PCR (RT-qPCR) in order to correlate the quantity of ATP and determine the cycle threshold (C_t) values, which reflect the bacterial population (CLas) within the insect. The DNA extraction was performed on the same perchloric acid extract used for ATP quantification. A 45- μ l aliquot of the perchloric acid extract was diluted to 1,100 μ l with extraction buffer (100 mM NaCl, 10 mM EDTA, 50 mM Tris [pH 9.0], 10 mM DTT), and the samples were centrifuged at 5,000 rpm for 1 min to remove the debris. A 20- μ l aliquot of 10% SDS was added to the recovered supernatant (1 ml), and the DNA was extracted as described above. Extracted DNA was used for RT-qPCR amplification using 16S rRNA primers HLBasf and HLBbr, the probe HLBp, TaqMan PCR master mix, SYBR green PCR master mix, and the protocol described by Li et al. (41) and Zhao et al. (42). Amplifications were performed in a 7500 RT-qPCR system, and supplies were from Applied Biosystems (Foster City, CA).

Total ATPase and GTPase activity. Five adult psyllids were placed in a 1-ml tube, 100 μ l of Tris buffer (10 mM Tris-HCl, 150 mM NaCl [pH 7.4]) was added, and the psyllids were crushed for 2 min on ice, as described above. The samples were centrifuged at $10,621 \times g$ for 5 min, and the supernatant was further filtered through a 10,000-molecular-weight-cutoff membrane (Millipore, Bedford, MA). Another 100 μ l of Tris buffer was added to the retentate, and the sample was centrifuged again to wash off the phosphate. The washing step was repeated, and the retentate was recovered in 50 μ l of Tris buffer. An aliquot of 20 μ l of the final sample was mixed with 20 μ l of assay buffer and 10 μ l of 4 mM ATP standard provided with the QuantiChrom ATPase/GTPase assay kit (Bioassay Systems, Hayward, CA) and placed in 96-well plate. The reaction mixture was incubated for 30 min at room temperature. A blank containing a 20 μ l of the enzyme extract was also mixed with 20 μ l of assay buffer and 10 μ l of Tris buffer and was run in the assay to determine the amount of phosphate background to be subtracted from the sample. At the end of the reaction time, 200 μ l of malachite green reagent was added to the reaction mixture and incubated for 30 min to terminate the enzyme reaction and generate the dark green color by reacting with free phosphate produced by ATPase/GTPase. The intensity of the stable dark green color was measured at 639 nm using a Synergy HT multimode microplate reader (Winooski, VT). The standard curve was constructed by incubating 50 μ l of phosphate standard (0, 15, 30, and 50 mM) with 200 μ l of malachite green reagent for 30 min and measured as mentioned above. All samples and standards were run in duplicate. Twenty-five healthy and 25 CLas-infected samples were analyzed, and each sample represented 5 psyllids. ATPase/GTPase activity was calculated according to the following formula: enzyme activity (in units per liter) = $([P_i] \times [RV]) / ([EV] \times [t])$, where P_i is the free phosphate produced from ATP and calculated from the standard curve (in micromolar concentration), RV is the reaction volume (50 μ l), EV is the enzyme volume used in the assay (20 μ l), and t is the reaction time (30 min). According to the ATPase/GTPase kit's manufacturer, one unit of activity is defined as the amount of enzyme that catalyzes the production of 1 μ M free phosphate per minute under the assay conditions.

Nucleotides and sugar nucleotide extraction from Asian citrus psyllid for HPLC analysis. Nucleotides and sugar nucleotides were extracted using perchloric acid, as described by Tomiya et al. (40), with slight modification. In brief, 60 Asian citrus psyllid adults were mixed with 200 μ l of ice-cold 5% perchloric acid and were crushed for 5 min in an ice bath using Kontes pestle. The samples were neutralized with potassium hydroxide and centrifuged at $10,621 \times g$ for 10 min. The samples were centrifuged again, and the supernatants were filtered through 10,000-molecular-weight-cutoff membranes. After adjusting to pH 7, the samples were centrifuged again, and the supernatant was kept at -20°C until analysis. Five replicates of each treatment were performed.

Nucleotide analysis by ion-pair reverse phase-HPLC. High-performance anion-exchange chromatography (HPAEC) was carried out using an Agilent 1200 series. HPLC was coupled to a diode array detector (HPLC-DAD) and a CarboPac PA100 column (Dionex, Sunnyvale, CA).

The following solvents were used as eluents: 1 mM sodium hydroxide (eluent 1 [E1]) and 1 M sodium acetate in 1 mM sodium hydroxide (eluent 2 [E2]). An aliquot of the *D. citri* extract (25 μ l) or a standard mixture was injected into the column equilibrated with a mixture (80:20 [vol/vol]) of E1 and E2. Elution was performed using E1 and E2, as described by Tomiya et al. (40) with slight modification, using the following gradient: elution time point T0 = 20% (vol/vol) E2, T10 = 20% (vol/vol) E2, T25 = 30% (vol/vol) E2, T35 = 40% (vol/vol) E2, T40 = 50% (vol/vol) E2, T45 = 60% (vol/vol) E2, T50 = 70% (vol/vol) E2, T55 = 70% (vol/vol) E2, T65 = 20% (vol/vol) E2, and T70 = 20% (vol/vol) E2. The flow rate for HPLC elution was 1 ml/min, and the column was kept at 30°C. Nucleotides and sugar nucleotides were detected by absorbance at 260 nm. Nucleotides and sugar nucleotides were identified by matching their retention times and UV-visible light spectra with the known standards. All of the nucleotides were quantified relative to their standards, and the unknown compounds were quantified relative to AMP. The adenylate energy charge was calculated using the following equation: $AEC = ([ATP] + 1/2[ADP])/([ATP] + [ADP] + [AMP])$ (43).

Survival assay. A 3-mm-thick blot paper (Bio-Rad, Hercules, CA) was placed in the bottom of each Corning Snap-Seal no. 1730 polypropylene container (height, 112 mm; outer diameter, 63 mm) (Fisher Scientific). The filter paper was saturated with 5 ml of 20% sucrose. Ten adult psyllids were introduced into each container, and the container was closed with clear plastic wrap. The psyllids were kept in temperature-controlled growth rooms (25 \pm 3°C, 60% \pm 5% RH, and a 16:8 [light/dark] photoperiod). The numbers of dead insects were recorded daily. The experiment contained five replicates each of healthy and CLas-infected psyllids. The experiment was repeated three times.

EPG. We used EPG methods to monitor *D. citri* feeding using two 4-channel monitors (described below). Each day, four psyllids from a noninfected (healthy) colony and four psyllids from a CLas-infected colony were monitored. After EPG, the four psyllids from the infected colony were tested for “*Candidatus Liberibacter asiaticus*” (CLas) using a 16S rRNA gene probe and primers (41). Only EPG recordings from psyllids that tested positive were used for the positive data, and only EPG recordings from the healthy colony were used for the CLas-negative data. The recordings from psyllids that tested negative for CLas (from the infected colony) were not analyzed. There were 28 recordings from healthy psyllids and 25 recordings from CLas-infected psyllids.

The equipment consisted of two alternating current/direct current (AC/DC) monitors (44), custom-built by William H. Bennett (EPG Equipment Co., Otterville, MO), operating in DC mode with 150 mV substrate voltage and 160 \times amplification. Data acquisition was through a DI710 AD converter (Dataq). A 2-cm-long, 24.5- μ m-diameter gold wire was attached to thoracic tergites of *D. citri* using silver glue (1:1:1 [wt/wt/wt] white glue-water-silver flake [8 to 10 μ m; Inframat Advanced Materials]). The other end of the gold wire was attached to a 23-mm-long, 0.48-mm-diameter copper wire using the same glue. This wire was soldered to a 20-mm-long, 1.14-mm-diameter brass nail that was inserted into the unit's head amp that was set to a resistance of 10⁹ Ω . Recordings were 24-h long. Midsweet orange scion on Kuharsky rootstock trees were obtained as resets from a commercial nursery, repotted, pruned to a height of 51 cm from the soil surface, and kept in a greenhouse in 3.92-liter black plastic pots measuring 18 cm at the rim and 18 cm deep filled with Fafard professional custom mix soil. Greenhouse lighting was supplemented using high-pressure sodium lighting to give 16 h:8 h photophase/scotophase. Plants were moved indoors to a Faraday cage constructed of a pure copper screen (0.15-mm-diameter wire, with 1 wire every 1.58 mm) attached to an aluminum frame. Illumination was provided by fluorescent bulbs, with room temperature maintained at 26.6°C. Humidity was not controlled. A psyllid colony was maintained in the same greenhouse using the same cultivar. All psyllids originated from a long-term colony that has been used in previous research (18, 45). The colony used in these tests required periodic infusions of psyllids from the original colony, but at least 1 week elapsed between colony augmentation and the removal of psyllids for experiments.

Gene expression analysis. The effects of CLas infection on psyllid genes, including ATP synthase α - and β -subunits mitochondrion-like (ATP synthase A and B), V-type proton ATPase catalytic subunit A (V-ATPase-V1a), the transitional endoplasmic reticulum ATPase (TER94), nucleotide diphosphate kinase (NDPK), and AMP-activated protein kinase α -subunit (AMPK-A) genes in *D. citri* adults, were evaluated using RT-qPCR as described by El-Shesheny et al. (23). The actin gene was used as a reference (endogenous gene) for comparing the relative levels of gene expression among treatments (46). Table 3 contains the primers used for gene expression.

Statistical analysis. Data were analyzed using JMP version 9.0 (SAS Institute, Inc.). Survival analysis was carried out using the Kaplan-Meier method. *P* values of log-rank tests were used for comparisons among the survival curves. A two-tailed *t* test was used to compare ATP levels, levels of ATPase activity, relative gene expression levels, and the mean concentrations of nucleotides and sugar nucleotides between healthy and CLas-infected *D. citri* colonies.

EPG results were analyzed using an SAS program that mimics the output of the Sarria Workbook, and 25 additional variables were added that focus on xylem feeding and the D waveform (Ebert 2.0 [<http://www.crec.ifas.ufl.edu/extension/epg/sas.shtml>]). The D waveform indicates that a psyllid has made contact with the phloem. There were 84 variables examined in total. These values were then transformed to mitigate issues with departures from normality. Durations were log transformed, counts were square root transformed, and percentages were arcsine square root transformed. Data were analyzed by mixed-model analysis of variance (ANOVA) using restricted maximum likelihood estimation (REML) (Proc Glimmix; SAS Institute, 2001).

TABLE 3 Primers used in gene expression for the selected genes in current study

Gene	Accession no.	Primer direction	Primer sequence	Reference or source
<i>hsp70</i>	XM_008482897	Forward	CGGTTATTACTGTCCCCGC	This study
		Reverse	TTGAATCACCCCAACAGAT	
ATP synthase A	XP_008482039	Forward	GGTATTCGTCCTATCAA	This study
		Reverse	GGCAGATCCTACACGGGATA	
V-ATPase-V1A	XP_008470205	Forward	CGAACTGGTACGAGTGGGAT	This study
		Reverse	GGATACCAGGACCAAGCTCA	
TER-94	XM_017447919.1	Forward	TGGAAACGGAAGACGAAGAC	This study
		Reverse	CCACCGGATTGACTCTGATT	
NDPK (<i>awd</i>)	ABG81980.1	Forward	AGAGGACTTGTGGGAAACATC	El-Shesheny et al. (23)
		Reverse	TGACAAAGACCAGGGAAGAAAG	
AMPK	XM_008486820.2	Forward	CCCCTAGTACAGGCAAACCA	This study
		Reverse	TGGAGAAGGACGAGGAGAGA	
Actin	XP-008468690	Forward	CCCTGGACTTGAACAGGAA	Tiwari et al. 2011 (46)
		Reverse	CTCGTGGATACCGCAAGATT	

The new variables that were added to the Sarria Workbook involving phloem contact were as follows: number of probes to first D, number of D, total duration of D, duration of nonprobing before first D, mean duration of D, average number of D per probe, time from first probe to first D, time from start of probe with first D to first D, number of probes after first D, number of probes <3 min after first D, number of D >10 min, time to first D >10 min, duration of longest D, and percent probing spent in D. The same set of variables was also calculated for G (xylem sap feeding), but three variables overlap existing Sarria variables. All EPG waveforms were interpreted by an experienced practitioner of EPG.

ACKNOWLEDGMENTS

We acknowledge the assistance of S. Jones and L. Lindsey with the psyllid colonies.

This work was supported by a grant from the Citrus Research and Development Foundation, Lake Alfred, FL, USA (grant 769-14).

REFERENCES

- Killiny N, Almeida RPP. 2009. Host structural carbohydrate induces vector transmission of a bacterial plant pathogen. *Proc Natl Acad Sci U S A* 106:22416–22420. <https://doi.org/10.1073/pnas.0908562106>.
- Lemon SM, Sparling PF, Hamburg MA, Relman DA, Choffnes ER, Mack A. 2008. Vector-borne diseases: understanding the environmental, human health, and ecological connections. Institute of Medicine (US) forum on microbial threats. National Academies Press, Washington, DC.
- Bové JM, Garnier M. 2002. Phloem- and xylem-restricted plant pathogenic bacteria. *Plant Sci* 163:1083–1098. [https://doi.org/10.1016/S0168-9452\(02\)00276-5](https://doi.org/10.1016/S0168-9452(02)00276-5).
- Nachappa P, Levy J, Pierson E, Tamborindeguy C. 2014. Correlation between “*Candidatus Liberibacter solanacearum*” infection levels and fecundity in its psyllid vector. *J Invertebr Pathol* 115:55–61. <https://doi.org/10.1016/j.jip.2013.10.008>.
- Stumpf CF, Kennedy GG. 2007. Effects of tomato spotted wilt virus isolates, host plants, and temperature on survival, size, and development time of *Frankliniella occidentalis*. *Entomol Exp Appl* 123:139–147. <https://doi.org/10.1111/j.1570-7458.2007.00541.x>.
- Nachappa P, Shapiro AA, Tamborindeguy C. 2012. Effect of “*Candidatus Liberibacter solanacearum*” on fitness of its vector, *Bactericera cockerelli* (Hemiptera: Trioziidae) on tomato. *Phytopathology* 102:41–46. <https://doi.org/10.1094/PHYTO-03-11-0084>.
- Manjunath KL, Halbert SE, Ramadugu C, Webb S, Lee RF. 2008. Detection of “*Candidatus Liberibacter asiaticus*” in *Diaphorina citri* and its importance in the management of citrus huanglongbing in Florida. *Phytopathology* 98:387–396. <https://doi.org/10.1094/PHYTO-98-4-0387>.
- Jagoueix S, Bové JM, Garnier M. 1994. The phloem-limited bacterium of greening disease of citrus is a member of the α -subdivision of the proteobacteria. *Int J Syst Bacteriol* 44:379–386. <https://doi.org/10.1099/00207713-44-3-379>.
- Tatineni S, Sagaram US, Gowda S, Robertson CJ, Dawson WO, Iwanami T, Wang N. 2008. *In planta* distribution of “*Candidatus Liberibacter asiaticus*” as revealed by polymerase chain reaction (PCR) and real-time PCR. *Phytopathology* 98:592–599. <https://doi.org/10.1094/PHYTO-98-5-0592>.
- Halbert SE, Manjunath KL. 2004. Asian citrus psyllids (Sternorrhyncha: Psyllidae) greening disease of citrus: a literature review and assessment of risk in Florida. *Fla Entomol* 87:330–353. [https://doi.org/10.1653/0015-4040\(2004\)087\[0330:ACPSPA\]2.0.CO;2](https://doi.org/10.1653/0015-4040(2004)087[0330:ACPSPA]2.0.CO;2).
- Reese J, Christenson MK, Leng N, Saha S, Cantarel B, Lindeberg M, Tamborindeguy C, MacCarthy J, Weaver D, Trease AJ, Ready SV, Davis VM, McCormick C, Haudenschield C, Han S, Johnson SL, Shelby KS, Huang H, Bextine BR, Shatters RG, Hall DG, Davis PH, Hunter WB. 2014. Characterization of the Asian citrus psyllid transcriptome. *J Genomics* 2:54–58. <https://doi.org/10.7150/jgen.7692>.
- Lin H, Gudmestad NC. 2013. Aspects of pathogen genomics, diversity, epidemiology, vector dynamics, and disease management for a newly emerged disease of potato: zebra chip. *Phytopathology* 103:524–537. <https://doi.org/10.1094/PHYTO-09-12-0238-RVW>.
- Duan Y, Zhou L, Hall DG, Li W, Doddapaneni H, Lin H, Liu L, Vahling CM, Gabriel DW, Williams KP, Dickerman A, Sun Y, Gottwald T. 2009. Complete genome sequence of citrus huanglongbing bacterium, “*Candidatus Liberibacter asiaticus*” obtained through metagenomics. *Mol Plant Microbe Interact* 22:1011–1020. <https://doi.org/10.1094/MPMI-22-8-1011>.
- Wang N, Trivedi P. 2013. Citrus huanglongbing: a newly relevant disease presents unprecedented challenges. *Phytopathology* 103:652–665. <https://doi.org/10.1094/PHYTO-12-12-0331-RVW>.
- Li W, Cong Q, Pei J, Kinch LN, Grishin NV. 2012. The ABC transporters in “*Candidatus Liberibacter asiaticus*.” *Proteins* 80:2614–2618. <https://doi.org/10.1002/prot.24147>.
- Vahling CM, Duan Y, Lin H. 2010. Characterization of an ATP translocase identified in the destructive plant pathogen “*Candidatus Liberibacter asiaticus*.” *J Bacteriol* 192:834–840. <https://doi.org/10.1128/JB.01279-09>.
- Galetto L, Bosco D, Balestrini R, Genre A, Fletcher J, Marzachi C. 2011. The major antigenic membrane protein of “*Candidatus Phytoplasma asteris*” selectively interacts with ATP synthase and actin of leafhopper vectors. *PLoS One* 6:e22571. <https://doi.org/10.1371/journal.pone.0022571>.
- Serikawa RH, Backus EA, Rogers ME. 2012. Effects of soil-applied imidacloprid on Asian citrus psyllid (Hemiptera: Psyllidae) feeding behavior. *J Econ Entomol* 105:1492–1502. <https://doi.org/10.1603/EC11211>.
- Colinet H. 2011. Disruption of ATP homeostasis during chronic cold stress and recovery in the chill susceptible beetle (*Alphitobius diaperi-*

- nus). *Comp Biochem Physiol Part A Mol Integr Physiol* 160:63–67. <https://doi.org/10.1016/j.cbpa.2011.05.003>.
20. Stenesen D, Suh JM, Seo J, Yu K, Lee KS, Kim JS, Min KJ, Graff JM. 2013. Dietary adenine controls adult lifespan via adenosine nucleotide biosynthesis and AMPK, and regulates the longevity benefit of caloric restriction. *Cell Metab* 17:101–112. <https://doi.org/10.1016/j.cmet.2012.12.006>.
 21. Apfeld J, O'Connor G, McDonagh T, DiStefano PS, Curtis R. 2004. The AMP-activated protein kinase AAK-2 links energy levels and insulin-like signals to lifespan in *C. elegans*. *Genes Dev* 18:3004–3009. <https://doi.org/10.1101/gad.1255404>.
 22. Curtis R, O'Connor G, DiStefano PS. 2006. Aging networks in *Caenorhabditis elegans*: AMP-activated protein kinase (aak-2) links multiple aging and metabolism pathways. *Aging Cell* 5:119–126. <https://doi.org/10.1111/j.1474-9726.2006.00205.x>.
 23. El-Shesheny I, Hijaz F, El-Hawary I, Mesbah I, Killiny N. 2015. Impact of different temperatures on survival and energy metabolism in the Asian citrus psyllid, *Diaphorina citri* Kuwayama. *J Insect Physiol* 192:28–37. <https://doi.org/10.1016/j.cbpa.2015.11.013>.
 24. Marazza D, Bornens P, Le Gal Y. 1996. Effect of ammonia on survival and adenylate energy charge in the shrimp *Palaemonetes varians*. *Ecotoxicol Environ Saf* 34:103–108. <https://doi.org/10.1006/eesa.1996.0050>.
 25. Picado AM, Le Gal Y. 1990. Assessment of industrial sewage impacts by adenylate energy charge measurements in the bivalve *Cerastoderma edule*. *Ecotoxicol Environ Saf* 19:1–7. [https://doi.org/10.1016/0147-6513\(90\)90072-D](https://doi.org/10.1016/0147-6513(90)90072-D).
 26. Sylvestre C, Le Gal Y. 1987. *In situ* measurements of adenylate energy charge and assessment of pollution. *Mar Pollut Bull* 18:36–39. [https://doi.org/10.1016/0025-326X\(87\)90656-4](https://doi.org/10.1016/0025-326X(87)90656-4).
 27. Hardie DG. 2011. AMP-activated protein kinase an energy sensor that regulates all aspects of cell function. *Genes Dev* 25:1895–1908. <https://doi.org/10.1101/gad.17420111>.
 28. Onyenwoke RU, Forsberg LJ, Liu L, Williams T, Alzate O, Brenman JE. 2012. AMPK directly inhibits NDKP through a phosphoserine switch to maintain cellular homeostasis. *Mol Biol Cell* 23:381–389. <https://doi.org/10.1091/mbc.E11-08-0699>.
 29. Johnson EC, Kazgan N, Bretz CA, Forsberg LJ, Hector CE, Worthen RJ, Onyenwoke R, Brenman JE. 2010. Altered metabolism and persistent starvation behaviors caused by reduced AMPK function in *Drosophila*. *PLoS One* 5:e12799. <https://doi.org/10.1371/journal.pone.0012799>.
 30. Schmid-Hempel P. 2005. Evolutionary ecology of insect immune defenses. *Annu Rev Entomol* 50:529–551. <https://doi.org/10.1146/annurev.ento.50.071803.130420>.
 31. Mayack C, Naug D. 2009. Energetic stress in the honeybee *Apis mellifera* from *Nosema ceranae* infection. *J Invertebr Pathol* 100:185–188. <https://doi.org/10.1016/j.jip.2008.12.001>.
 32. Aliferis AK, Copley T, Jabaji S. 2012. Gas chromatography-mass spectrometry metabolite profiling of worker honey bee (*Apis mellifera* L.) hemolymph for the study of *Nosema ceranae* infection. *J Insect Physiol* 58:1349–1359. <https://doi.org/10.1016/j.jinsphys.2012.07.010>.
 33. Martín-Hernández R, Meana A, Prieto L, Salvador AM, Garrido-Bailón E, Higes M. 2007. Outcome of colonization of *Apis mellifera* by *Nosema ceranae*. *Appl Environ Microbiol* 73:6331–6338. <https://doi.org/10.1128/AEM.00270-07>.
 34. Martini X, Hoffmann M, Coy MR, Stelinski LL, Pelz-Stelinski KS. 2015. Infection of an insect vector with a bacterial plant pathogen increases its propensity for dispersal. *PLoS One* 10:e0129373. <https://doi.org/10.1371/journal.pone.0129373>.
 35. Ojcius DM, Degani H, Mispelter J, Dautry-Varsat A. 1998. Enhancement of ATP levels and glucose metabolism during an infection by Chlamydia. NMR studies of living cells *J Biol Chem* 273:7052–7058. <https://doi.org/10.1074/jbc.273.12.7052>.
 36. Ramsey JS, Johnson RS, Hoki JS, Kruse A, Mahoney J, Hilf ME, Hunter WB, Hall DG, Schroeder FC, MacCoss MJ, Cilia M. 2015. Metabolic interplay between the Asian citrus psyllid and its *Proffettella* symbiont: an Achilles' heel of the citrus greening insect vector. *PLoS One* 10:e0140826. <https://doi.org/10.1371/journal.pone.0140826>.
 37. Vyas M, Fisher TW, He R, Nelson W, Yin G, Cicero JM, Willer M, Kim R, Kramer R, May GA, Crow JA, Soderlund CA, Gang DR, Brown JK. 2015. Asian citrus psyllid expression profiles suggest *Candidatus* Liberibacter asiaticus-mediated alteration of adult nutrition and metabolism, and of nymphal development and immunity. *PLoS One* 10:e0130328. <https://doi.org/10.1371/journal.pone.0130328>.
 38. Pelz-Stelinski KS, Killiny N. 2016. Better together: association with "*Candidatus* Liberibacter asiaticus" increases the reproductive fitness of its insect vector, *Diaphorina citri* (Hemiptera: Liviidae). *Ann Entomol Soc Am* 109:371–376. <https://doi.org/10.1093/aesa/saw007>.
 39. Gahnim M, Fattah-Hosseini S, Levy A, Cilia M. 2016. Morphological abnormalities and cell death in the Asian citrus psyllid (*Diaphorina citri*) midgut associated with *Candidatus* Liberibacter asiaticus. *Sci Rep* 6:33481. <https://doi.org/10.1038/srep33481>.
 40. Tomiya N, Ailor E, Lawrence SM, Betenbaugh MJ, Lee YC. 2001. Determination of nucleotides and sugar-nucleotides involved in protein glycosylation by high performance anion-exchange chromatography: sugar nucleotide contents in cultured insect cells and mammalian cells. *Anal Biochem* 293:129–137. <https://doi.org/10.1006/abio.2001.5091>.
 41. Li WB, Hartung JS, Levy L. 2006. Quantitative real-time PCR for detection and identification of *Candidatus* Liberibacter species associated with citrus huanglongbing. *J Microbiol Methods* 66:104–115. <https://doi.org/10.1016/j.mimet.2005.10.018>.
 42. Zhao Q, Xie S, Sun Y, Chen Y, Gao J, Li H, Wang X, Syed SF, Liu B, Wang L, Zhang G, Zhou E-M. 2015. Development and evaluation of a SYBR Green real-time RT-PCR assay for detection of avian hepatitis E virus. *BMC Vet Res* 11:195. <https://doi.org/10.1186/s12917-015-0507-5>.
 43. Chapman AG, Fall L, Atkinson DE. 1971. Adenylate energy charge in *Escherichia-coli* during growth and starvation. *J Bacteriol* 108:1072–1086.
 44. Backus EA, Bennett WH. 2009. The AC-DC correlation monitor: new EPG design with flexible input resistors to detect both R and emf components for any piercing-sucking hemipteran. *J Insect Physiol* 55:869–884. <https://doi.org/10.1016/j.jinsphys.2009.05.007>.
 45. Tiwari S, Mann RS, Rogers ME, Stelinski LL. 2011. Insecticide resistance in field populations of Asian citrus psyllid in Florida. *Pest Manag Sci* 67:1258–1268. <https://doi.org/10.1002/ps.2181>.
 46. Tiwari S, Gondhalekar AD, Mann RS, Scharf ME, Stelinski LL. 2011. Characterization of five CYP4 genes from Asian citrus psyllid and their expression levels in *Candidatus* Liberibacter asiaticus-infected and uninfected psyllids. *Insect Mol Biol* 20:733–744. <https://doi.org/10.1111/j.1365-2583.2011.01103.x>.